An ecological model for the Scheldt Estuary and tidal rivers ecosystem Spatial and temporal variability of plankton

Naithani, J.; de Brye, B.; Buyze, E.; Vyverman, W.; Legat, Vincent; Deleersnijder, Eric

DOI
10.1007/s10750-016-2710-1

Publication date
2016

Document Version
Accepted author manuscript

Published in
Hydrobiologia: the international journal on limnology and marine sciences

Accepted for publication in "Hydrobiologia"
(20 February 2016)

An ecological model for the Scheldt Estuary and tidal rivers ecosystem: spatial and temporal variability of plankton

J. Naithani[1,*], B. de Brye[1], E. Buyze[2], W. Vyverman[2], V. Legat[1], and E. Deleersnijder[3,4]

[1] *Université catholique de Louvain, Institute of Mechanics, Materials and Civil Engineering (IMMC), 4 Avenue G. Lemaître, B-1348 Louvain-la-Neuve, Belgium*

[2] *Section Protistology and Aquatic Ecology, Department of Biology, University of Ghent, K.L. Ledeganckstraat 35, 9000 Ghent, Belgium*

[3] *Université catholique de Louvain, Institute of Mechanics, Materials and Civil Engineering (IMMC) & Earth and Life Institute (ELI), 4 Avenue G. Lemaître, B-1348 Louvain-la-Neuve, Belgium*

[4] *Delft University of Technology, Delft Institute of Applied Mathematics (DIAM), Mekelweg 4, 2628CD Delft, The Netherlands*

[*] *Corresponding author: jaya.naithani@uclouvain.be*

February 2016

Abstract

This paper presents the formulation, structure and governing equations of an ecosystem model developed for the Scheldt estuary and the tidal river network. The model has twelve state variables: nitrate, ammonium, phosphate, dissolved silica, freshwater and marine phytoplankton (chlorophytes and diatoms), freshwater zooplankton (ciliates, rotifers and copepods) and benthic detritus. The ecological model is coupled to the 1-D tidal resolving version of the Second-generation Louvain-la-neuve ice-ocean Model (SLIM)[1]. The model successfully simulates the observed longitudinal and seasonal variation of plankton in the Scheldt estuary. The phytoplankton production in the estuary is governed by temperature, underwater available light, turbidity, nutrients and discharge. Of all these factors, discharge seems to be dominant. High discharge increases the turbidity in the water column and thus reduces the underwater light, while low discharge means decreased nutrients. The marine phytoplankton species were present as far to the upstream limits of the brackish waters, with diatoms dominating in the spring and chlorophytes in early summer. The freshwater phytoplankton are seen from late spring to

[1]http://www.climate.be/SLIM.

summer. Freshwater zooplankton followed the evolution of freshwater phytoplankton.

Key words: ecological model; SLIM, Scheldt estuary; tidal river; chlorophytes; diatoms; ciliates; rotifers; copepods

Introduction

Originating from France, the Scheldt river flows through Belgium, enters the Netherlands and discharges into the North Sea (Figure 1). In Belgium its main tributaries are Dender, Durme and Rupel. The Scheldt estuary is a macro-tidal estuary, extending from the mouth at Vlissingen (0 km) to Ghent (160 km) (Chen et al., 2005; Meire et al 2005). The tidal wave is semidiurnal. The mean tidal range at Vlissingen is 4.5 m, 5.85 m near Antwerp (78.5 km) and 2 m near Ghent (Van Rijn, 2010). The tidal wave also enters its major tributaries Rupel (and its tributaries: Dijle, Zenne, Kleine Nete, Grote Nete) and Durme (Meire et al., 2005). The estuary has extensive salty (Western Scheldt, >15 PSU, 0 to around 55 km), brackish (Sea Scheldt, $0.5 - 15$ PSU, between around 55 to 90 km) and freshwater (Upper Sea Scheldt, <0.5 PSU from around 90 km) tidal reaches (Chen et al., 2005; Meire et al., 2005; Dijkman & Kromkamp, 2006). The extent of salinity intrusion strongly

depends on the freshwater discharge. During high discharge (from around November till March) periods, the transect up to around 58 km from the mouth consists of freshwater (< 0.5 PSU). The salinity gradient along the length of the estuary effects the freshwater as well as the marine plankton (Muylaert et al., 1997; 2000a; Muylaert & Sabbe, 1999; Koeman et al., 2004; Lionard et. al., 2005a; Dijkman & Kromkamp, 2006). The salinity stress (osmotic) is seen to increase their respiration (Flameling & Kromkamp, 1994; Griffin et al., 2001; Lionard et. al., 2005a).

Another important characteristic of the whole Scheldt estuary is the high water column turbidity (Baeyens et al., 1998; Chen et al., 2005; Gazeau et al., 2005; Kromkamp & Peene, 1995, 2005; Dijkman & Kromkamp, 2006; Gourge et al., 2013). According to Baeyens et al. (1998) and Dijkman & Kromkamp, (2006) the zone from 55 km to 78 km from the sea corresponding roughly with the salinity zone from 10 to 2 psu, is the zone of highest turbidity. High turbidity results in high values of light attenuation and decreases photosynthesis in spite of high nutrients (Cloern, 1987; Muylaert et at., 1997, 2005a; Chen et al., 2005; Kromkamp & Peene, 1995, 2005; Dijkman & Kromkamp, 2006; Brion et al., 2008). The zone of high turbidity also corresponds to high salinity zone for freshwater species and low salinity zone for marine species, thereby reducing their growth in this region.

Ecological models for the Scheldt river estuary range from very simple to

more complex ones. With time both kind of models continue to be developed. Soetaert et al. (1994) and Soetaert & Herman (1995) developed an ecosystem model to study the phytoplankton production, nitrogen dynamics and carbon flows, respectively in the Westerschelde. Desmit et al. (2005) presented a zero-dimensional model for phytoplanktonic production of the complete 160 km tidal Scheldt estuary from Vlissingen until Ghent. They investigated how short-term, tidally driven physical forcings interfere with the incident sunlight energy to sustain phytoplankton production in the nutrient-rich, well-mixed tidal estuary. Using a simple light-limited primary production model to estimate phytoplankton growth rates in the freshwater tidal reaches of the Scheldt estuary Muylaert et al. (2005a) observed two phytoplankton blooms in the freshwater tidal reaches, one in March and another one in July-August. According to them the first bloom, which was situated in the upstream reaches of the freshwater tidal zones, was imported from the river Scheldt and the second bloom, which was situated more downstream in the freshwater tidal reaches, appeared to have developed within the estuary. Vanderborght et al. (2002; 2007) proposed a reactive-transport model to investigate nutrients and carbon budgets of the estuary. Arndt et al. (2007; 2009) presented a two-dimensional, nested grid, hydrodynamic, and reactive-transport model of the estuary and its tributaries. Hofmann et al. (2008) constructed a 1-D, biogeochemical, pelagic, reactive-transport model of the mixed, turbid,

heterotrophic Scheldt estuary. Other studies include a phytoplankton production model incorporating an increasingly complex description of underlying biological mechanisms such as intracellular fluxes and microbial loop (Arndt et al., 2011; Gypens et al., 2012).

This study presents a one-dimensional ecological model of the entire Scheldt river estuary. The ecosystem model simulates the dominant phytoplankton and zooplankton groups observed in the Scheldt estuary, particularly in the upper freshwater reaches. The chemical and biological processes are simulated for the tidal Scheldt and its tributaries extending from Vlissingen near the mouth of the estuary to Ghent. The ecosystem model is coupled to SLIM (see below for a short explanation). The aim of this study is to provide a detailed description of the biological processes contained in the ECO-SLIM model along with the simulations for the year 2003.

The Model

The domain

The model domain (Fig. 1) consists of the entire Scheldt estuary from Vlissingen (0km) until Ghent (160km). This includes a river network comprising of the Scheldt river and its bifurcation (the Lys) at Ghent, the Rupel and its tributaries (the

Dijle, the Zenne, the Nete, the Grote Nete and the Kleine Nete), the Durme and the Dender. The Scheldt estuary in divided into three different zones: the saline lower estuary, the brackish upper estuary and the freshwater tidal river. The lower estuary extends along 55 km from the mouth near Vlissingen to the Dutch-Belgian border. The width of the estuary is 8 km at the mouth and decreases gradually to about 1.5 km near the Dutch-Belgian border. The tidal amplitude increases in this section (from 1.75 at the mouth to 2 m at Bath for the $M2$ component of the tide) due to bank convergence, shallow areas and partial reflexion. The lower estuary is influenced by strong tidal mixing. The upper estuary is about 38 km long extending from the Dutch-Belgian border to Rupelmonde, where its width is reduced to 100 m. This part is somewhat stratified from time to time (Winterwerp et al., 2003). In this section, the $M2$ tidal amplitude increases up to 2.3 m to the south of Antwerp, then decreases slightly upstream. Finally, the freshwater tidal riverine zone, extending from Hemiksem to sluices near Ghent (where its width reduces to 50 m). In this part river banks are well defined and the tidal amplitude decreases gradually because of dissipative processes (the amplitude of $M2$ tide is about 1 m at the Ghent sluices).

The physical model (SLIM)

The physical model consists of 1D cross-section integrated mass and momentum conservation equations (de Brye et al., 2010). The model is based on the 1D shallow

water equations with varying cross section. The downstream boundary lies at the mouth of estuary, located around Vlissingen. The M2 and S2 tides are imposed here according to the observation for Vlissingen. In the upstream of the model, far from the tidal influence, near Ghent and at the extremities of the main tidal rivers network, daily averaged discharges are imposed. The details about the SLIM model and the parameterization can be found in de Brye et al. (2010).

Ecological model

The ecological model (Figure 2) simulates four dissolved inorganic nutrients: nitrate ($NO3$), ammonia ($NH4$), phosphate ($PO4$) and dissolved silica (DSi). Phytoplankton ($PHYTO$) module includes freshwater chlorophytes (CHL), marine chlorophytes ($CHLM$), freshwater diatoms (DIA) and marine diatoms ($DIAM$). Zooplankton module (ZOO) consists of ciliates (CIL) and rotifers (ROT) as micro-zooplankton, and copepods (COP) as meso-zooplankton. These are the dominant plankton groups found in the freshwater tidal reaches of the Scheldt estuary (Muylaert and Sabbe, 1999; Muylaert et al., 2000a; 2009; Lionard et al., 2005a; Dijkman and Kromkamp, 2006; Lionard et al., 2008a; Tackx et al., 2004). Only freshwater zooplankton are simulated in the model. The marine zooplankton are not simulated. Macro-zooplankton or planktivorous-fish are not explicitly modelled but its influence in terms of predation pressure on other zooplankton is

taken into account and is used as the closure term.

Growth in the model is a function of the availability of light, nutrients and temperature. Respiration is influenced by a salinity function. This term acts to increase the rate of respiration as the salinity changes above/below an optimum salinity for freshwater/marine planktons. Parameterization for respiration in the model includes activity and maintenance respiration (Weger et al., 1989; Langdon 1993; Krompkamp & Peene, 1995). The activity respiration depends on the gross production, whereas the maintenance respiration depends on total biomass. All biological rates in the model are doubled when temperature increases by 10 °C (Eppley, 1972; Kremer & Nixon, 1978). For marine diatoms a different temperature function is used. This temperature function ensures a spring and late summer high biomass as measured in the upstream parts of the estuary and the North Sea (Fransz & Verhagen, 1985; Admiraal, 1977; Montagnes & Franklin, 2001; Baretta et al., 2009).

Zooplankton graze only on freshwater phytoplankton (marine zooplankton are not simulated). Excretion and respiration of organisms and the remineralisation of the detritus are added directly to the inorganic nutrient pool. A small percentage of faeces and dead organic matter is immediately remineralised to inorganic nutrients, while the rest contributes to the detrital pool and is defined as particulate organic

matter (POM) in the model. The direct regeneration is a function of temperature and represents the effect of the microbial food web, which is not explicitly included in the model. The POM settles to the sediments. The model is closed by predation by macrozooplankton/zooplanktivorous fish. Predation on zooplankton by fish is defined similarly to grazing on phytoplankton by zooplankton. For predation, the fish biomass is considered similar to copepod biomass.

The general equation describing a nonconservative variable is defined as:

$$\frac{\partial}{\partial t}(A\ \mathrm{VAR}) + \frac{\partial}{\partial x}(Au\mathrm{VAR} - Ak\frac{\partial \mathrm{VAR}}{\partial x}) = A\ R_{\mathrm{VAR}} \tag{1}$$

where VAR can be any model dependent variable such as $PHYTO$, ZOO, nutrients, POM and BD. The left-hand side terms represent any local change in the VAR and advection and diffusion of the VAR. The right-hand side of the equation represents the biological rates of the VAR. Biological variables (except for nutrients) are expressed in units of concentration of carbon (μgCl^{-1}).

Biological rates effecting the local change in phytoplankton are growth, respiration, extracellular excretion, mortality and grazing.

$$R_{PHYTO} = GROWTH_{PHYTO} - RESP_{PHYTO} - ECE_{PHYTO} - MORT_{PHYTO} - GRAZ_{PHYTOZOO} \quad (2)$$

186

187 Phytoplankton growth rate, $GROWTH_{PHYTO}$ ($\mu gCl^{-1}d^{-1}$), is considered to be
188 influenced by nutrients, light intensity and temperature.

$$GROWTH_{PHYTO} = GROWTH_{mPHYTO} * min(F(N), F(I)) * F(T) * PHYTO \quad (3)$$

189

190 where $GROWTH_{mPHYTO}$ is the maximum growth rate constant (d^{-1}) of
191 phytoplankton at 0 °C. $F(N)$ describes the effect of nutrients availability.

192

193 The effect of nutrients, $F(N)$, on growth is modelled according to Michaelis-Menten
194 formulation. The nitrogen limitation includes a "gourmet term of ammonium"
195 (preference of phytoplankton for ammonia over nitrate, Wroblewski, 1977). The
196 nutrient dependency is defined as:

$$F(N) = min\Bigg[\Big(\frac{NO_3}{NO_3 + K_{NO_3PHYTO}} exp(-\Psi NH4) + \frac{NH_4}{NH_4 + K_{NH_4PHYTO}}\Big), \Big(\frac{PO_4}{PO_4 + K_{PO_4PHYTO}}\Big), \Big(\frac{Si}{Si + K_{SiPHYTO}}\Big)\Bigg] \quad (4)$$

197

198 The constants and parameters are defined in Table 2. Ψ is the ammonium inhibition
199 coefficient. Silica limitation acts only on diatoms.

200

201 Light limitation to growth, $F(I)$, is modelled as an exponential decrease of light
202 intensity with depth (Lambert–Beer's equation). This is defined as:

$$F(I) = \frac{1}{k_e H}\left(arctan\frac{I_o}{2I_k} - arctan\left(\frac{I_o \exp^{(-k_e H)}}{2I_k}\right)\right) \quad (5)$$

203

204 The light attenuation coefficient $k_e = k_{e1} + k_{e2} * SPM$. k_{e1} is the background
205 attenuation and k_{e2} is the specific contribution of SPM.

The temperature-dependent term, $F(T)$, is defined using the "Q_{10}" relation:

$$F(T) = e^{(k_T T)} \tag{6}$$

Temperature function for marine diatoms is defined as:

$$F(T_{DIAM}) = e^{(-(T-Topt_{DIAM})^2/(wt_{DIAM})^2)} \tag{7}$$

Respiration rate, $RESP$ ($\mu gCl^{-1}d^{-1}$), of phytoplankton depends on temperature and salinity stress. It is defined as:

$$RESP_{PHYTO} = \Big(RESP_{b0} * F(T)_{RESP} * PHYTO + RESP_{p0} * GROWTH_{PHYTO})\Big) * F(S) \tag{8}$$

The term $F(S)$ is the respiration response to salinity. For freshwater-adapted phytoplankton it is $F(S)_{fresh} = 1.07^S$. For marine or saltwater-adapted phytoplankton it is $F(S)_{marine} = 1 + 5 * 0.85^S$. The respiration rate increases as

219 salinity increases/decreases for freshwater/saltwater species, and, therefore, the
220 growth declines.

221

222 Extracellular excretion rate of phytoplankton, ECE ($\mu gCl^{-1}d^{-1}$), is defined as:

223

$$ECE_{PHYTO} = k_{ECE} * GROWTH_{PHYTO} \tag{9}$$

224

225 Mortality rate, $MORT$ ($\mu gCl^{-1}d^{-1}$), is the loss of phytoplankton by natural death
226 and is defined as a quadratic equation and depends on temperature.

227

$$MORT_{PHYTO} = MORT_{PHYTO0} * F(T) * PHYTO * PHYTO \tag{10}$$

228

229 Loss of phytoplankton by grazing is described after the zooplankton equation.
230 Equations similar to (2) are written for CHL, $CHLM$, DIA and $DIAM$.

231

232 The rates effecting the local change in zooplankton are grazing, respiration,
233 excretion, fecal pellet, mortality and predation.

$$R_{ZOO} = GRAZ_{PHYTOZOO} - RESP_{ZOO} - EXC_{ZOO} - FEC_{ZOO} - MORT_{ZOO} - PRED_{ZOOZOO} \quad (11)$$

234

235 The first term is the grazing of phytoplankton by zooplankton, second and third
236 terms represent the respiration and metabolic excretion, fourth term formulates
237 egestion of fecal pellets by zooplankton and fifth term represent the loss due to
238 mortality. The last term is the predation on zooplankton by other zooplankton
239 groups. This term is a loss term for both ciliates and rotifers, and, for copepods it
240 is a gain term.

Grazing rate, $GRAZ$ ($\mu gCl^{-1}d^{-1}$), is described with a temperature-dependent term (Q_{10}) and an Ivlev equation with a fixed feeding threshold (Ivlev, 1945; Parsons et al., 1967). $PHYTO_{min}$ is the threshold below which zooplankton do not graze.

$$GRAZ_{PHYTOZOO} = max\Big(0, g_{maxPHYTOZOO} * F(T) * \left[1 - e^{-\lambda*(PHYTO_{min}-PHYTO)}\right] * ZOO\Big) \quad (12)$$

241

242 $g_{maxPHYTOZOO}$ is the maximum grazing rate constant, (d^{-1}). Marine phytoplankton
243 species are not grazed.

244

245 Respiration rate of zooplankton is defined as: $RESP_{ZOO} = RESP_{ZOO0} * F(S)_{fresh} *$
246 $F(T)_{RESP} * ZOO$, excretion rate is defined as: $EXC_{ZOO} = n_{eZOO} * GRAZ_{PHYTOZOO}$
247 and the egestion of fecal pellets is defined as: $FEC_{ZOO} = n_{fZOO} * GRAZ_{PHYTOZOO}$.
248 Mortality of zooplankton is defined with the similar expression as that for
249 phytoplankton. Equations similar to (11) are written for freshwater CIL, ROT
250 and COP.

251

252 The nutrients equation include the uptake by phytoplankton, the metabolic loss
253 terms of all biological variables, a percentage of their mortality, a percentage of feces
254 of zooplankton, and the remineralized detritus.

$$
\begin{aligned}
R_{NUT} = \sum_{PHYTO=1}^{4} \Big[& -GROWTH_{PHYTO} + RESP_{PHYTO} \\
& + ECE_{PHYTO} + p_{MORT} * MORT_{PHYTO} \Big] / R_{C:NUT} \\
& + \sum_{ZOO=1}^{3} \Big[EXC_{ZOO} + RESP_{ZOO} + p_{FEC} * FEC_{ZOO} \\
& + p_{MORT} * MORT_{ZOO} \Big] / R_{C:NUT} \\
& + r_D * F(T_{rem}) * (POM + BD) / R_{C:NUT}
\end{aligned} \tag{13}
$$

$R_{C:NUT}$ is the ratio of carbon to respective nutrient in the plankton. Equations similar to 13 are written for $NO3$, $NH4$, $PO4$ and DSi. Silica equation includes the biological terms only from diatoms, rotifers and copepods. The $(-GROWTH + RESP)$ term in $NO3$ equation is multiplied by (RN_{PHYTO}), while in the $NH4$ equation this term is multiplied by $(1 - RN_{PHYTO})$. (RN_{PHYTO}) is the ratio of nitrate uptake to total nitrogen uptake for phytoplankton and is defined as: $RN_{PHYTO} = \frac{\frac{NO_3}{(NO_3+K_{NO_3PHYTO})} exp(-\Psi NH4)}{\frac{NO_3}{(NO_3+K_{NO_3PHYTO})} exp(-\Psi NH4) + \frac{NH_4}{(NH_4+K_{NH_4PHYTO})}}$. Nitrification and denitrification processes are modelled as simple first order processes affected only by temperature. Nitrification of ammonia is parameterized as: $NIT = NIT_0 * F(T) * NH_4$. Denitrification is defined as: $DENIT = DENIT_0 * F(T) * NO_3$. Nitrification of ammonia is added to the $NO3$

equation.

Particulate organic matter or pelagic detritus (μgCl^{-1}), is formed mainly by dead organic matter and zooplankton feces, the rest of what is not directly remineralized in the water column.

$$
\begin{aligned}
R_{POM} = & \sum_{PHYTO=1}^{4} (1 - p_{MORT}) * MORT_{PHYTO} \\
& + \sum_{ZOO=1}^{3} \Big[(1 - p_{MORT}) * MORT_{ZOO} \\
& + (1 - p_{FEC}) * FEC_{ZOO} \Big] \\
& - REM_{POM} - SED_{POM}
\end{aligned} \tag{14}
$$

where REM_{POM} is the rate of decomposition of POM defined as $r_D * F(T)_{rem} * POM$ and SED_{POM} is the POM sedimenting to the bottom defined as $-(w_{sPOM}/H) * POM$. Decomposed inorganic nutrients are released back into the water column.

Benthic detritus ($mgCm^{-2}$), in the sediments is formed mainly by settling of POM/pelagic detritus out of the water column. It is decomposed to further release

the dissolved inorganic nutrients to the water column.

$$R_{BD} = H * \left[SED_{POM} - \frac{REM_{BD}}{H} \right] \tag{15}$$

REM_{BD} is the decomposition rate of BD defined as $r_{Ds} * F(T_{rem}) * BD$.

The parameter values used in the model (Table 2) are derived from literature or calibrated within literature ranges. These literature ranges are discussed here. The range of maximum growth rate constants of phytoplankton at 20 °C is 0.5 d^{-1} - 5 d^{-1} (Parsons et al., 1984). The values for the half saturation constants for nutrients uptake used here are within the range found in the literature (Di Toro et al., 1971; Di Toro, 1980; Fransz & Verhagen, 1985; Muylaert et. al., 2000b; Kishi et. al., 2007). k_{e1} is chosen to be the summer value given by Fransz & Verhagen (1985). Light saturation constant ranges from $20 - 300$ μE m^{-2} s^{-1} (Ignatiades & Smayda, 1970; Montagnes & Franklin, 2001). The basic respiration is a function of total biomass (0 - 10 %) and the activity respiration depends on production (30 - 55 %) (Laws & Caperon, 1976; Kromkamp & Peene, 1995; Soetaert et al., 1994). About 5% of the production in phytoplankton is excreted in soluble form

(Mague et al., 1980; Fransz & Verhagen, 1985). Kremer & Nixon (1978) show that maximum grazing rate constant values lie in the range of 0.10 - 2.50 d^{-1}. Tackx (1987) and Klepper et al. (1994) estimated that the range of maximum grazing rate constants of zooplankton at 15 °C is 0.5 - 2.0 d^{-1}. For the Ivlev constant, Kremer & Nixon (1978) reported the range of 0.4 - 25.0 $(mgC/l)^{-1}$. All Q_{10}-values are approximately 2, except the one for remineralization that is about 3 (Fransz and Verhagen, 1985). This is because the bacterial growth in the Scheldt estuary is among the highest reported in the literature (Goosen et al. 1995). All rate constants are defined at 0 °C. Fractions of mortality and fecal pellets remineralized directly in the water column and contributing to the inorganic nutrient pool is considered to be 40 %. Sedimentation of POM used in the literature varies from $1 - 1.5\ m\ d^{-1}$ (Smetacek, 1980; Fransz & Verhagen, 1985; Blauw et al., 2009). The mineralization rate coefficient used for POM is 0.12 d^{-1}. The same rate was adapted for the bottom sediments/benthic detritus. Nitrification and denitrification rates are taken from Blauw et al. (2009). Carbon to nutrient ratios are taken from Lingeman-Kosmerchock (1978), Los (1982), Fransz & Verhagen (1985).

Model forcing

For the Scheldt and its tributaries, upstream discharges are interpolated from daily averaged data from the Hydrological Information Center (HIC, 2015). The discharge

316 of the Ghent–Terneuzen canal are interpolated from the daily averaged data collected
317 by the Netherlands institute for inland water management and treatment (RWS,
318 2015). Discharge is a time dependent forcing. The water discharge of the river
319 Scheldt (Figure 3) and its tributaries (not shown) show a pronounced seasonal cycle,
320 with high flow occurring in early winter and low in summer. Because of the strong
321 correlation between discharge and the phytoplankton growth observed in the Scheldt
322 estuary (Muylaert et al., 2001, 2005a, 2005b; Arndt et al., 2007; Lionard et al 2008b),
323 daily discharge is applied on the boundary of all the tributaries of the Scheldt.

324 The incident light intensity, water temperature and SPM are given as
325 time-dependent external forcing. Water temperature and solar radiation (Figure 4)
326 are obtained from (Waterbase, 2015; Scheldtmonitor, 2015; NCEP, 2015). Maximum
327 temperature was observed in the month of August while solar insolation was at
328 its maximum in the month of June. SPM in the estuary shows large spatial and
329 seasonal variation (Chen et al., 2005; Desmit et al., 2005; Lionard et al., 2005a;
330 2008b; Muylaert et al., 2005a; 2005b; Arndt et al., 2007; Gourge, 2011). SPM was
331 interpolated using the data from (NIOO, 2015) and above mentioned literature.

332 Initial and boundary conditions

333 Monthly plankton values for the tributaries are sparse, therefore, a constant value
334 of biological state variables (1 μgCl^{-1}) was considered for initial as well as for the

boundary conditions. Winter values of nutrients for the year 2003 were considered as the boundary conditions (Van der Zee et al., 2007; Carbonnel et al., 2009; ScheldtMonitor). These values were applied at the boundaries of all the rivers and at Vlissingen. Winter averaged boundary values were applied as the initial conditions for these nutrients. The salinity is set to 33 at its marine boundary (Vlissingen) and to 0 at the freshwater boundary at Ghent and at the boundaries of all the rivers. A spin-up of one year was considered before the actual simulation, once the parameters were fixed. The model is not found to be sensitive to the initial phytoplankton values, since the simulation starts in January and the first bloom starts in spring, giving enough time for the biology to establish.

Results

Figure 5 shows the longitudinal variation of model simulated and measured salinity averaged over the year 2003. Starting from around 33 pps at Vlissingen, the annual averaged salinity reduces to around 2 pps at 90 km from the sea. Salinity is significant in the freshwater tidal zone during summer, when the discharge is at its minimum.

The ecological model captured the basic features of the Scheldt river estuary, notably, the spatial and seasonal gradients in various variables (Figures 6 - 8). These

variations are discussed in the following sections.

Phytoplankton

Freshwater phytoplankton biomass (Figures 6a, 6c, 7a and 7c) starts developing in June when the light and temperature conditions start becoming favorable for growth. It is seen from around 50 km to around 150 km. Because of relatively higher discharge in June the maximum biomass is displaced further downstream to around 90 km (Figures 6a and 6c). Afterwards as the discharge decreases the biomass increases. The maximum freshwater phytoplankton biomass is seen in August upstream of 120 km (Figures 6a and 6c). During this period the water temperature was maximal and the discharge was minimal. Because of low discharge and low SPM, the light penetration in the water column was high. The saline intrusion during low discharge might also be responsible for the freshwater biomass being constrained to more upstream locations. The maximum freshwater biomass occurs in summer (June-September), when all the necessary conditions for growth (nutrients, light, temperature, salinity and discharge) are at their optimum level (Figures 6a, 6c, 7a and 7c).

Sudden decrease in biomass in early July and early September, (Figures 6a, 6c, 7a and 7c) in the freshwater phytoplankton in spite of favorable light and temperature conditions, cannot be accounted for only by grazing. This might

be because of the consumption of already low levels of nutrients because of low discharge.

Marine phytoplankton are seen as far up to the brackish zones (Figures 6b, 6d, 7b and 7d). Marine diatoms start developing from April onwards and show their peak biomass in May and decrease afterwards, while marine chlorophytes are seen in summer with a maximum in July.

Likewise to phytoplankton carbon, the chlorophyll*a* concentration was highest in the freshwater zone, decreased in the brackish zone and showed secondary maxima in the marine waters (Figures 6j and 7j). Primary production was highest in summer in the freshwater upstream parts, while it was highest in spring near the mouth of the estuary (Figures 6a - 6c and Figures 7a - 7d). During late autumn growth is limited because of increased discharge and unfavorable light and temperature conditions.

Zooplankton

The freshwater zooplankton community followed the evolution of freshwater phytoplankton in time and space (Figures 6e, 6g, 6i, 7e, 7g and 7i). They were found from late spring to the beginning of autumn, being maximum in summer. They are high in the upstream parts in late summer and have lower biomass in late spring and early summer and are displaced further downstream. Their abundance decreased downstream near Antwerp. Copepods show higher abundance than ciliates but much

less than those of rotifers. Ciliate abundance (Figures 6e and 7e) stays relatively constant compared to rotifers and copepods (Figures 6g, 6i, 7g and 7i), since they are quickly grazed down upon by rotifers. This imply the top-down control of rotifers on ciliates in summer.

Particulate organic matter and Benthic detritus

The POM (mainly carbon) is present only in the spring and summer as a result of planktons in the estuary (Figures 6f and 7f). Benthic detritus (Figures 6h and 7h) depends on the POM formation and river discharge. The deposition of benthic detritus is present throughout the growth season, around June-September in the freshwater parts and in the spring near the sea. High discharge leads to the reduction of its deposition. They both (POM and BD) decrease in autumn and disappear afterwards.

Nutrients

The evolution of nutrients (Fiigure 8) is in agreement with measurements. Nutrients in the estuary are being supplied continuously from the river Scheldt and its tributaries except for a small time, when they are consumed in the upstream regions of the Scheldt in late spring and summer. During this period the supply of nutrients is already low because of low discharge. Nutrients level increase again in autumn,

when the discharge increases. After this time the photosynthetic activity reduces because of low temperature and low light environment. Another minima in the nutrients is observed in the downstream areas around 30 km in summer because of the consumption by marine phytoplankton species. However, in these downstream locations they continue to stay low in autumn.

Sensitivity analysis

Model sensitivity was tested for a few parameters found crucial for the plankton biomass along the length of the Scheldt estuary.

Effect of irradiance

The tests with changes in I_{kPHYTO} are summarised in Figure 9 and Table 3. Increasing the optimum light intensity for chlorophytes decreased their biomass and increased the biomass of freshwater diatoms. Increasing the optimum light intensity for diatoms decreased their biomass and increased the biomass of freshwater chlorophytes. While the biomass of marine chlorophytes remain unchanged. Increasing the optimum light intensity simultaneously for chlorophytes and diatoms, increased the biomass of freshwater diatoms only. The biomass of ciliates/rotifers decreased/increased for all the three cases, while the biomass of copepods increased only for the first case and decreased for the rest two cases. These tests imply that

light can be a crucial limiting factor for growth in summer.

Effect of fish predation

Reducing the biomass of planktivorous fish, increased the biomass of copepods. Biomass of marine species and ciliates remain unchanged, while the biomass of the other planktons decreased. Although fish has no direct influence on the biomass of chlorophytes, its biomass too is reduced (Figure 10). The increased biomass of copepods increased the grazing pressure on other plankton. The amount of carbon grazed by copepods was much higher than the amount of increased biomass of copepods in carbon. This might have reduced the losses (mortality, respiration, excretion, etc.) and the nutrient regeneration by them. This in turn further reduced the biomass of plankton other than copepods.

Discussion

Freshwater phytoplankton are separated by their marine counterparts by a salinity range which is too high for the growth of freshwater species and too low for the growth of marine species. Salinity alone, however, is not responsible for the disappearance of phytoplankton biomass in the brackish waters around 90 km from Vlissingen. The depth of the estuary is maximum around Antwerp. It is the low light conditions in the deeper waters along with high SPM concentration that makes

445 them disappear in the brackish waters.

446 The absence of freshwater plankton biomass in early spring might be because
447 of almost zero initial boundary values of the biomass and because of the absence
448 of transport from the river Scheldt. According to Muylaert et al. (2000a) the
449 phytoplankton in the uppermost parts of the estuary near Ghent are the ones
450 imported from the river Scheldt, the import being more important in spring than in
451 summer. This import is considered negligible in the present study.

452 Phytoplankton blooms were able to develop in the upper estuary in summer
453 in spite the high rotifer populations and their strong grazing impact. Implying
454 the dominance of discharge over grazing, in shaping the phytoplankton blooms.
455 However, the fact that rotifers graze equally on phytoplankton, detritus and ciliates
456 might also account to its high values in the Scheldt and less detrimental influence to
457 phytoplankton blooms. Most of the riverine input of nutrients are depleted either
458 by consumption or by dilution in the upstream reaches of the Scheldt.

459 In conclusion the model simulated the observed seasonal blooms of
460 phytoplankton and zooplankton production. The longitudinal variation in the
461 variables indicates the influence of salinity, SPM and discharge, while the seasonal
462 variation is influenced by temperature, light and discharge. Longitudinal and
463 seasonal input of the data in the present study is considered constant and is set

at a non-zero minimum value. The initial boundary conditions seem to be playing a role in the space-time evolution of the simulations. This is evident in the absence of biomass at the extreme boundaries. In future it is envisaged to perform the simulations using the seasonal variation of all the state variables as initial values at the boundaries of all the rivers and at the mouth of the estuary. This will take care of the winter-spring biomass of zooplankton and the spring freshwater phytoplankton biomass transported from the rivers to the estuary, mainly from the Ghent river (Muylaert et al., 2000a; Lionard et al., 2005b; Carbonnel et al., 2009).

The Scheldt estuary ecosystem experiences a very high frequency variations of the physical parameters. It is very difficult to separate/define the influence of one forcing parameter independently of the other. Each parameter influences in a special way in the presence or absence of other parameter. Their dominance is difficult to be interpreted or defined at times. On the contrary each has its well defined role.

Acknowledgements

The author Jaya Naithani is grateful to Dr Klaas Deneudt for all the help provided in locating the data. Thanks are also due to the two reviewers for their careful, critical and constructive comments. This research was conducted in the framework of the Interuniversity Attraction Pole TIMOTHY (IAP VI. 13), funded by Belgian

Science Policy (BELSPO), and the project "Taking up the challenge of multi-scale marine modelling", which is funded by the Communauté Française de Belgique under contract ARC10/15-028 (Actions de recherche concertées) with the aim of developing and applying SLIM. Computational resources were provided by the supercomputing facilities of the Université catholique de Louvain (CISM/UCL) and the Consortium des Equipment de Calcul Intensif en Féderation Wallonie Bruxelles (CECI) funded by the Fond de la Recherche Scientifique de Belgique (FRS-FNRS).

References

[1] Arndt, S., Regnier, P., & J.-P. Vanderborgth, 2009. Seasonally-resolved nutrient export fluxes and fluxes and filtering capacites in a macro tidal estuary. Journal of Marine Systems, 78, 42-58.

[2] Arndt, S., Vanderborgth, J.-P., & P. Regnier, 2007. Diatom growth response to physical forcing in a macrotidal estuary: coupling hydrodynamics, sediment transport and biogeochemistry. Journal of Geophysical Research 12 doi:10.1029/2006JC003581.

[3] Arndt, S., G. Lacroix, N. Gypens, P. Regnier & C. Lancelot, 2011. Nutrient dynamics and phytoplankton development along the estuary-coastal zone continuum: A model study. Journal of Marine Systems, 84, 49-66.

[4] Baeyens, W., B. van Eck, C. Lambert, R. Wollast & L. Goeyens, 1998. General description of the Scheldt estuary. Hydrobiologia, 366, 1-14.

[5] Blauw, A.N., H.F.J. Los, M. Bokhorst & P.L.A. Erftemeijer, 2009. GEM: a genetic ecological model for estuaries and coastal waters, Hydrobiologia, 618, 175-198.

[6] Brion, N., Andersson, M.G.I., Elskens, M., Diaconu, C., Baeyens, W., Dehairs, F., & J.J. Middelburg, 2008. Nitrogen cycling, retention and export in a eutrophic temperate macrotidal estuary. Marine Ecological Progress Series, 357, 87-99.

[7] Carbonnel, V., M. Lionard, K. Muylaert & L. Chou, 2009. Dynamics of dissolved and biogenic silica in the freshwater reaches of a macrotidal estuary (The Scheldt, Belgium). Biogeochemistry, 96, 49-72.

[8] Chen, M.S., Wartel, S., Van Eck, B., & D.V. Maldegem, 2005. Suspended matter in the Scheldt Estuary. Hydrobiologia, 540, 79-104.

[9] Cloern, J.E., 1987. Turbidity as a control on phytoplankton biomass and productivity. Continental Shelf Research, 7, 1367-1381.

[10] de Brye, B., A. de Brauwere, O. Gourgue, T. Kärnä, J. Lamprechts, R. Comblen & E. Deleersnijder, 2010. A finite-element, multi-scale model of the Scheldt tributaries, river, estuary and ROFI, Coastal Engineering, doi:10.1016/j.coastaleng.2010.04.001.

[11] Desmit, X., Vanderborght, Regnier, P., & R. Wollast, 2005. Control of phytoplankton production by physical forcing in a strongly tidal, well-mixed estuary. Biogeosciences, 2, 205-218.

[12] Dijkman, N. & J.C. Kromkamp, 2006, Photosynthesis characteristics of the phytoplankton in the Scheldt estuary: community and single-cell fluorescence measurements. European Journal of Phycology, 41, 425-434.

[13] Di Toro, D.M., D.J. O'Connor & R.V. Thomann, 1971. A dynamic model of the phytoplankton population in the Sacramento-San Joaquin Delta. Advances

in Chemistry Series, Non-equillibrium Systems in Natural Water Chemistry, 106, Americal Chemical Society, Washington, D.C., 131-180.

[14] Di Toro, D.M., 1980. Applicability of cellular equillibrium and monod theory to phytoplankton growth kinetics. Ecological Modelling, 8, 201-218.

[15] Eppley, R. W., 1972. Temperature and phytoplankton growth in the sea. Fishery Bulletin, 70: 1063-1085.

[16] ESRL, 2015. http://www.esrl.noaa.gov/psd/data/gridded/data.ncep.reanalysis2.html.

[17] Flameling, I. A. & J. Kromkamp, 1994. Responses of respira- tion and photosynthesis of Scenedesmus protuberans Fritsch to gradual and steep salinity increases. Journal of Plankton Research 16: 1781–1791.

[18] Fransz, H.G. & J.H.G. Verhagen, 1985. Modelling research on the production of phytoplankton in the southern bight of the north sea in relation to riverborne nutrient loads. Netherlands Journal of Sea Research, 19, 241-250.

[19] Gazeau, F., Gattuso, J.-P., Middelburg, J.J., Brion, N., Schiettecatte, L.-S., Frankignouille & A.V. Borges, 2005. Planktonic and whole system metabolism in a nutrient-rich estuary (the Scheldt Estuary). Estuaries, 28, 868-883.

[20] Goosen, N.K., P. van Rijswijk & U. Brockmann, 1995. Comparison of heterotrophic bacterial production rates in early spring in the turbid estuaries of the Scheldt and the Elbe. Hydrobiologia, 311, 31-42.

[21] Gourge, O., 2011. Finite element modelling of sediment dynamics in the Scheldt. PhD Thesis, UCL, pp. 151.

[22] Gourge, O. W. Baeyens, M.S. Chen, A. de Brauwere, B. de Brye, E. Deleersnijder, M. Elskens & V. Legat, 2013. A depth-averaged two-dimensional sediment transport model for environmental studies in the Scheldt Estuary and tidal river netsork. Journal Marine Systems, 128, 27-39.

554 [23] Gypens, N., E. Delhez , A. Vanhoutte-Brunier, S. Burton , V.
555 Thieu, P. Passy, Y. Liu, J. Callens, V. Rousseau, & C. Lancelot,
556 2012. Modelling phytoplankton succession and nutrient transfer along the
557 Scheldt estuary (Belgium, The Netherlands). Journal of Marine Systems.
558 http://dx.doi.org/10.1016/j.jmarsys.2012.10.006.

559 [24] HIC, 2015. http://www.hydra.vlaanderen.be/hic/servlet/index.

560 [25] Hofmann, A.F., K. Soetaert, & J.J. Middelburg, 2008. Present nitrogen and
561 carbon dynamics in the Scheldt estuary using a novel 1-D model. Biogeosciences,
562 5, 981-1006.

563 [26] Ignatiades, L. & T.J. Smayda, 1970. Autecological studies on the marine
564 diatom Rhizosolenia fragilissima Bergon. I. The influence of light, temperature
565 and salinity. Journal of Phycology, 6, 332-33.

566 [27] IRMB (Institut Royal Meteorologique de Belgique) (2003– 2004) Bulletins
567 mensuels, Observations climatologiques, parties I et II. Institut Royal
568 Meteorologique de Belgique, Bruxelles (In French/Dutch).

569 [28] Ivlev, V.S., 1945. The biological productivity of waters. Usp. soverm. Biol., 19,
570 98-120.

571 [29] Klepper, O., M.W.M. van der Tol, H. Scholten, & P.M.J. Herman, 1994.
572 SMOSES: a simulation model for the Oosterschelde ecosystem. Hydrobiologia,
573 282:283, 437-451.

574 [30] Koeman, R.P.T., Brochard, C.J.E., Fockens, K., Verweij, G.L., & Esselink, P.,
575 2004. Biomonitoring van Fytoplankton in de Nederlandse Zoute Wateren 2003
576 Kite Diagrammen, Koeman en Bijkerk, Ecologisch onderzoek en advies, Haren:
577 The Netherlands.

578 [31] Kremer, J.N. & S.W. Nixon, 1978. A Coastal Marine Ecosystem: Simulation
579 and Analysis. Ecological Studies, vol. 24. Springer-Verlag, Heidelberg, p. 217.

[32] Kromkamp, J.C. & J. Peene, 1995. Possibility of net phytoplankton primary production in the turbid Schelde estuary (SW Netherlands). Marine Ecology Progress Series, 121, 249-259.

[33] Kromkamp, J.C. & J. Peene, 2005. Changes in phytoplankton biomass and primary production between 1991 and 2001 in the Westerschelde estuary (Belgium/The Nederlands). Hydrobiologia, 540, 117-126.

[34] Langdon C., 1993. The signficance of respiration production measurements based on both carbon and oxygen. In. L1 WKW, Maestrini SY (eds) Measurement of primary productlon from the molecular to the global scale. Vol 197 ICESS MSS, lnternatlonal Council for the Exploration of the Sea, Copenhagen, p 69-78.

[35] Laws.E. & J. Caperon, 1976. Carbon and nitrogen metabolism by Monochrysis lutheri: measurement of growth-rate dependent respiration rates. Marine Biology, 36, 85-97.

[36] Lingeman-Kosmerchock, M., 1978. Phytoplankton cells, their nutrient contents, mineralisation and sinking rates. Delft Hydraulics Laboratoty report R1310, Delft.

[37] Lionard, M., Muylaert, K., van Gansbeke, D. & W. Vyverman, 2005a. Influence of changes in salinity and light intensity on growth of phytoplankton communities from the Schelde river estuary (Belgium/The Netherlands). Hydrobiologia, 540, 105-115.

[38] Lionard, M., Azémar, F., Boulêtreau, Muylaert, K., Tackx, M. & W. Vyverman, 2005b. Grazing by meso- and microzooplankton on phhytoplankton in the upper reaches of the Schelde estuary (Belgium/The Netherlands). Estuarine, Coastal and Shelf Science, 64, 764-774.

[39] Lionard, M., Muylaert, K., Tackx, M. & W. Vyverman, 2008a. Evaluation of the per formance of HPLC-CHEMTAX analysis for determining phytoplankton

605 biomass and composition in a turbid estuary (Schelde, Belgium). Estuarine,
606 Coastal and Shelf Science, 76, 809-817.

607 [40] Lionard, M., Muylaert, K., Hanoutti, A., Maris, T., Tackx, M. & W. Vyverman,
608 2008b. Inter-annual variability in phytoplankton summer blooms in the freshwater
609 tidal reaches of the Schelde estuary (Belgium), Estuarine, Coastal and Shelf
610 Science, 79, 694-700.

611 [41] Los, F.J., 1982. Mathematical simulation of algae blooms by the model BLOOM
612 II. Delft Hydraulics Laboratory Publ. no 316, Delft.

613 [42] Meire, P., T. Ysebaert, S. van Damme, E.V. den Bergh, T. Maris & E. Struyf,
614 2005. The Scheldt estuary: a description of a changing ecosystem. Hydrobiologia,
615 540, 1-11.

616 [43] Muylaert, K., Van Kerckvoorde, A., Vyverman, W. & K. Sabbe, 1997.
617 Structural characteristics of phytoplankton assemblages in tidal and non-tidal
618 freshwater systems: a case study from the Schelde basin, Belgium. Freshwater
619 Biology, 38, 263–276.

620 [44] Muylaert, K. & K. Sabbe, 1999. Spring phytoplankton assemblages in and
621 around the maximum turbidity zone of the estuaries of the Elbe (Germany), the
622 Schelde (Belgium/The Netherlands) and the Gironde (France). Journal of Marine
623 Systems, 22, 133–149.

624 [45] Muylaert, K., Sabbe, K. & W. Vyverman, 2000a. Spatial and temporal
625 dynamics of phytoplankton communities in a freshwater tidal estuary (Schelde,
626 Belgium). Estuarine, Coastal and Shelf Science, 50, 673–687.

627 [46] Muylaert, K., Mieghem, R.V., Sabbe, K., Tackx, M. & W. Vyverman, 2000b.
628 Dynamics and trophic roles of heterotrophic protists in the plankton of a
629 freshwater tidal estuary. Hydrobiologia, 432, 25-36.

[47] Muylaert, K., Van Wichelen, J., Sabbe, K., & W. Vyverman, 2001. Effects of freshets on phytoplankton dynamics in a freshwater tidal estuary (Schelde, Belgium). Archiv für Hydrobiologie 150, 269-288.

[48] Muylaert, K., M. Tackx & W. Vyverman, 2005a. Phytoplankton growth rates in the freshwater tidal reaches of the Schelde estuary (Belgium) estimated using a simple light-limited primary production model. Hydrobiologia, 540, 127-140.

[49] Muylaert, K., R. Dasseville, L. De Brabandere, F. Dehairs & W. Vyverman, 2005b. Dissolved organic carbon in the freshwater tidal reaches of the Schelde estuary. Estuarine, Coastal and Shelf Science, 64, 591-600.

[50] Muylaert, K., Sabbe, K. & W. Vyverman, 2009. Changes in phytoplankton diversity and community composition along the salinity gradient of the Schelde estuary (Belgium/The Netherlands). Estuarine, Coastal and Shelf Science, 82, 335-340.

[51] NCEP, 2015. http://www.esrl.noaa.gov/psd/data/gridded/data.ncep.reanalysis2.html.

[52] Parsons, T.R., Le Brasseur, R.J. & J.D. Fulton, 1967. Some observations on the dependence of zooplankton grazing on cell size and concentration of phytoplankton blooms. Journal of Oceanographical Society of Japan, 23, 10-17.

[53] Parsons, T.R., Takahashi, M., & B. Hargrave, 1984. Biological Oceanographic Processes, third ed. Pergamon Press.

[54] RWS, 2015. Ministerie van Verkeer en Waterstaat, www.waterbase.nl.

[55] ScheldtMonitor, Onderzoek Milieu-effecten Sigmaplan. Multidisciplinaire studie rond het estuariene milieu van de Zeeschelde. Ecosystem Management Research Group, UA; Protistology and Aquatic Ecology, Ugent; Laboratoire d'Ecologie des Hydrosystèmes, Université Paul Sabatier - France, i.o.v. Vlaamse Overheid; Beleidsdomein Mobiliteit en

655 Openbare Werken; Waterwegen en zeekanaal NV, metadata available at
656 http://www.scheldemonitor.be/imis.php?module=dataset&dasid=1381.

657 [56] Smetacek, V.S, 1980. Zooplankton standing stock, copepod faecal pellets and
658 particulate detritus in Kiel Bight. Marine Biology, 63, 1-11.

659 [57] Soetaert, K. Herman, P.M.J. & J. Kromkamp, 1994. Living in twilight:
660 estimating net phytoplankton growth in the Westerschelde estuary (The
661 Netherlands) by means of an ecosystem model (MOSES). Journal of Plankton
662 Research, 16, 1277-1301.

663 [58] Soetaert, K. & P.M.J. Herman, 1995. Carbon flows in the Westerschelde
664 estuary (TheNetherlands) evaluated by means of an ecosystem model (MOSES).
665 Hydrobiologia, 311: 247-266.

666 [59] Tackx, M. L . M ., 1987 . Grazing door zooplankton in de Oosterschelde . Ph .
667 D . thesis, Lab . voor ecologie en systematiek, Vrije Universiteit Brussel.

668 [60] Tackx, M. L. M., N. de Pauw, R. van Mieghem, F. Azemar, A. Hannouti, S.
669 van Damme, F. Fiers, N. Daro, & P. Meire, 2004. Zooplankton in the Schelde
670 estuary, Belgium and The Netherlands. Spatial and temporal patterns, Journal
671 of Plankton Research, 26, 133– 141.

672 [61] Van der Zee, C., N. Roevros, & L. Chou, 2007. Phosphorus speciation,
673 transformation and retention in the Scheldt estuary (Belgium/The Netherlands)
674 from the freshwater tidal limits to the North Sea. Marine Chemistry, 106, 76-91.

675 [62] Vanderborght, J.P., Wollast, R., Loijens, M., & P. Regnier, 2002. Application
676 of a transport-reaction model to the estimation of biomass fluxes in the Scheldt
677 estuary. Biogeochemistry, 59, 207-237.

678 [63] Vanderborght, J.P., Folmer, I.M., Agiuilera, D.R. Unhrenholdt, T., &
679 P. Regnier, 2007. Reactive-transport modelling of C, N, and O_2 in a

river-estuarine-coastal zone system: Application to the Scheldt estuary, Marine Chemistry, 106, 92-110.

[64] Van Rijn, L.C., 2010. Tidal phenomena in the Scheldt Estuary. Report, Deltares, pp 105.

[65] Waterbase, 2015. Ministerie van Verkeer en Waterstaat, www.waterbase.nl.

[66] Weger, H. G., Herzig, R., Falkowski, P. G., & D.H. Turpin, 1989. Respiratory losses in the light in a marine diatom: measurements by short-term mass spectrometry, Limnology and Oceanography, 34, 1153–1161.

[67] Wroblewski, J.S., 1977. A model of phytoplankton plume formation during variable Oregon upwelling. Journal of Marine Research, 35, 357-394.

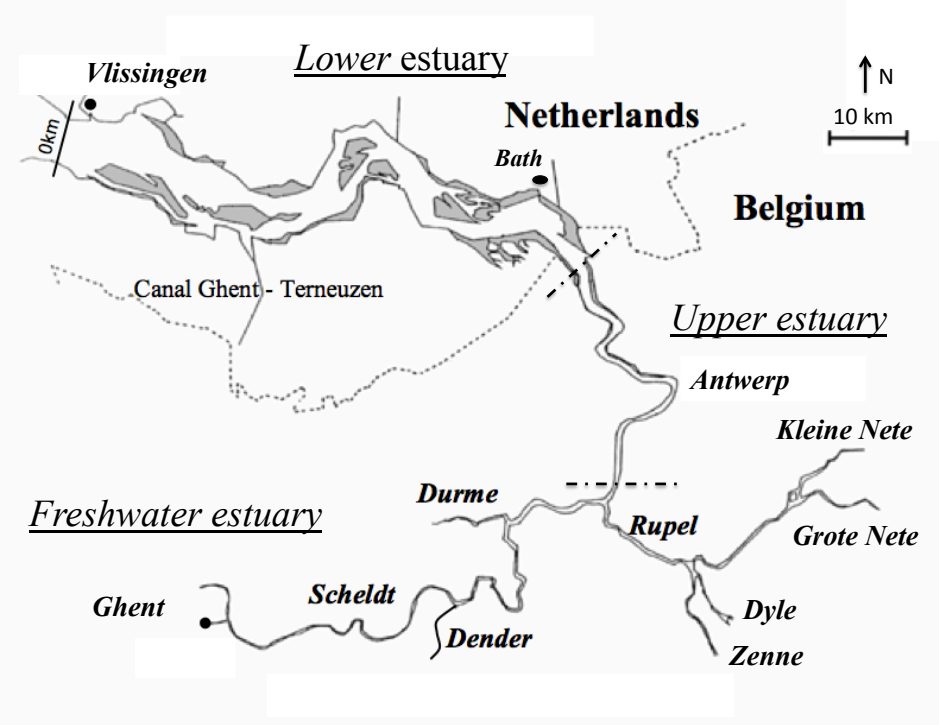

Figure 1: Map of the Scheldt river estuary and its tributaries. The three zones of the estuary (lower, upper and freshwater) are separated by dash-dot lines.

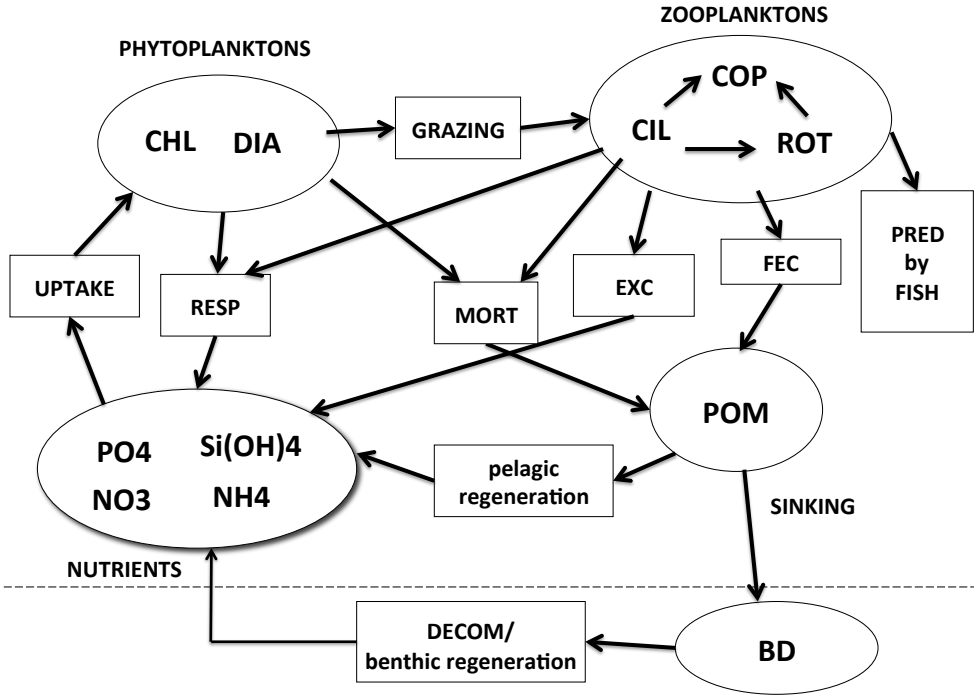

Figure 2: Schematic view of the ECO-SLIM model showing various variables (circles) and processes (boxes) in the model.

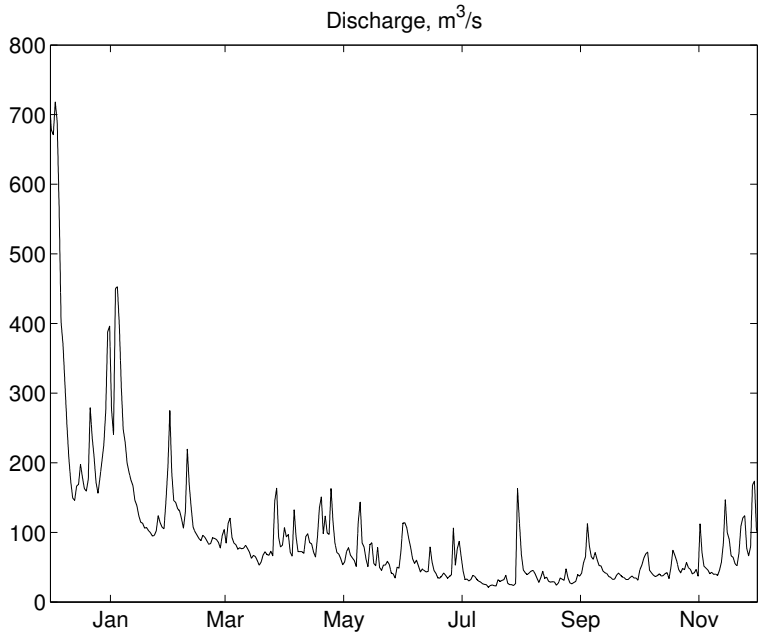

Figure 3: Discharge of the river Scheldt for the year 2003.

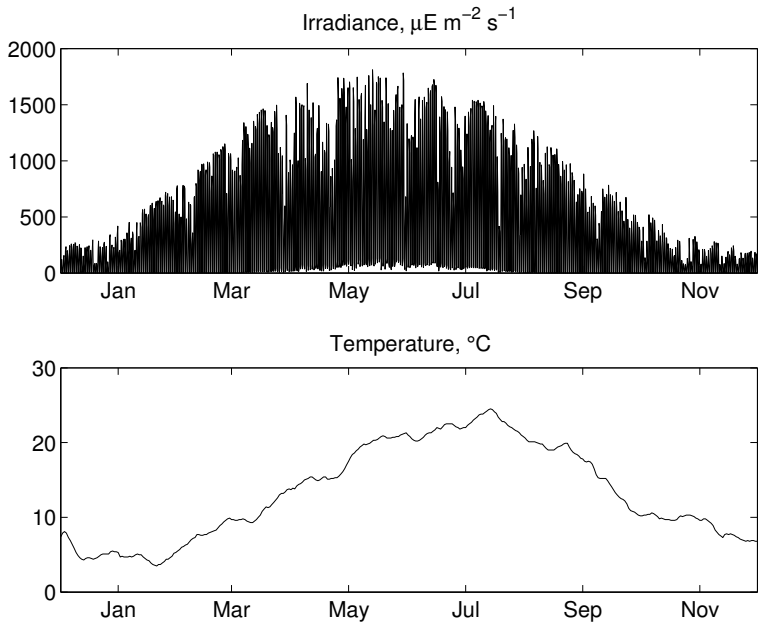

Figure 4: Irradiance and temperature for the year 2003.

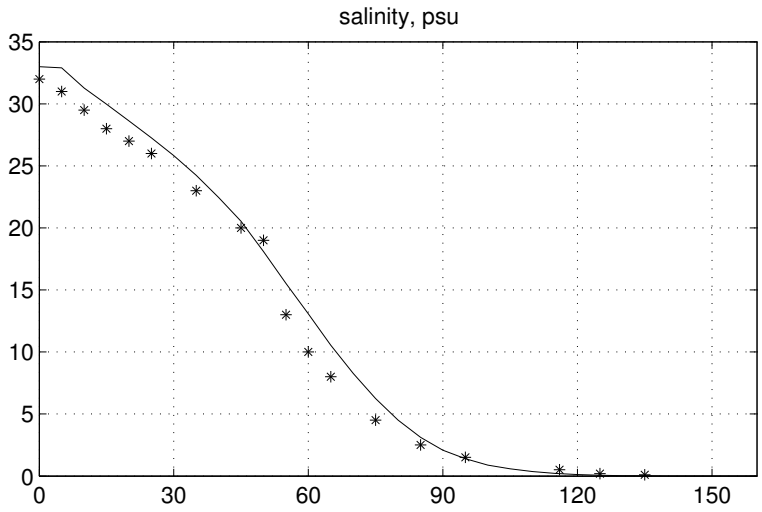

Figure 5: Longitudinal variation of the model simulated salinity (-) and measured salinity (*) for the year 2003. X-axis is in kms, with 0 km at Vlissingen and 160 km at Ghent.

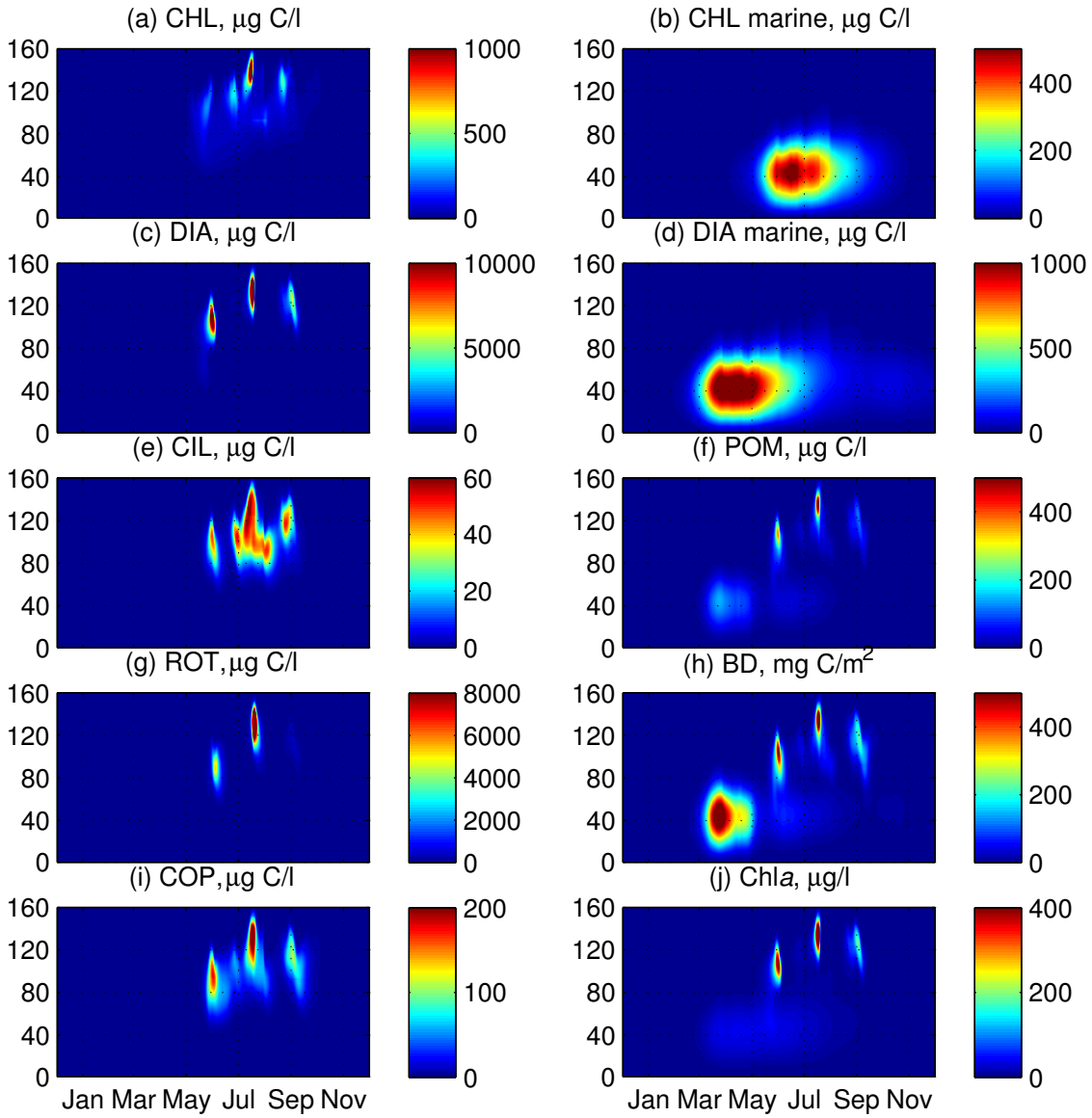

Figure 6: The spatio-temporal variation of model simulated variables for the year 2003. Y-axis is in kms, with 0 km at Vlissingen and 160 km at Ghent. The three main rivers Rupel, Durme and Dender join the Scheldt river at around 92, 100 and 123 kms, respectively from Vlissingen.

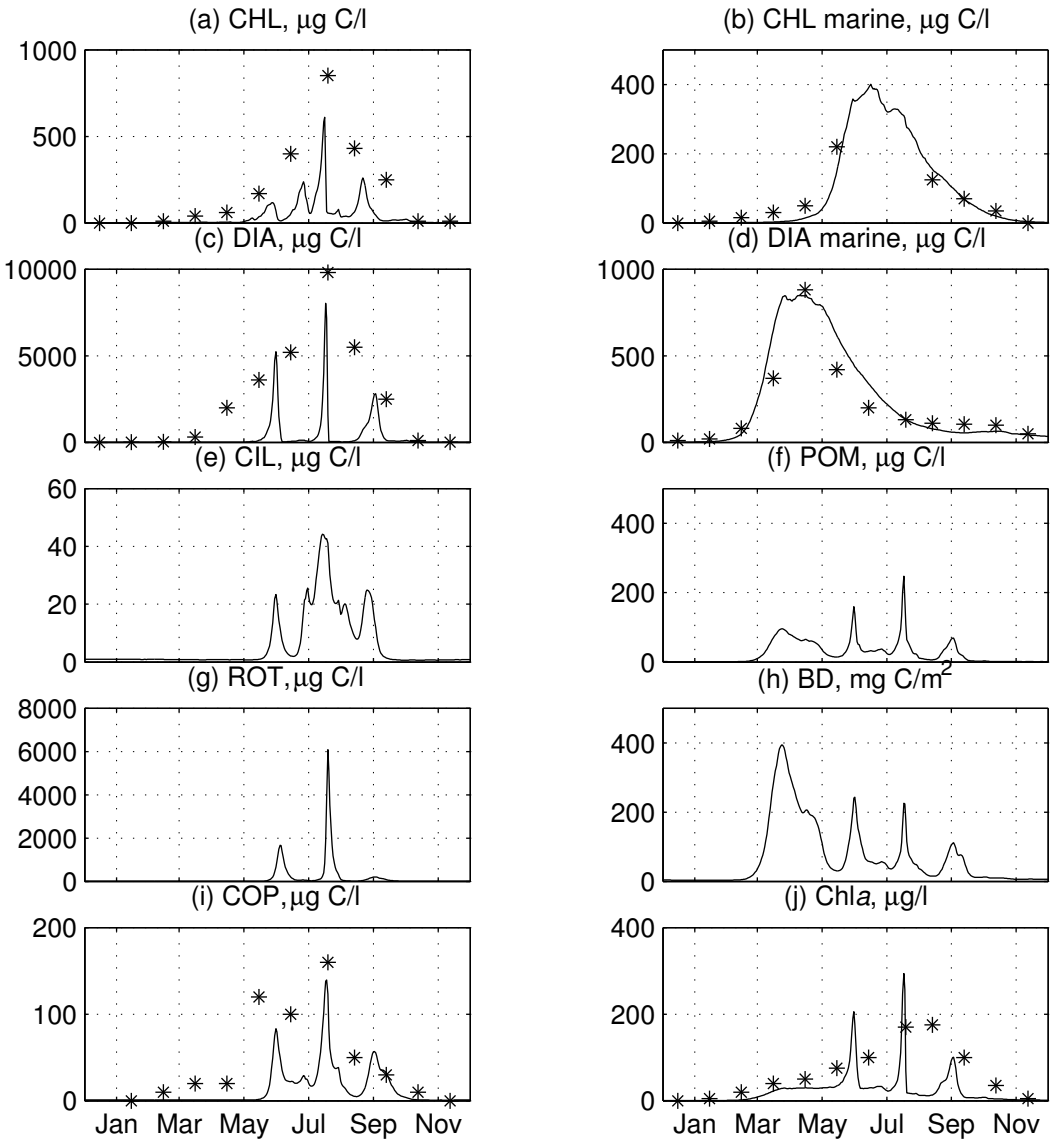

Figure 7: Temporal variation of model simulated variables (-) and measurements (*) for the year 2003. Freshwater plankton are averaged over the freshwater estuary and the marine phytoplankton are averaged over the marine parts, organic waste and chlorophyll-a are averaged over the whole estuary.

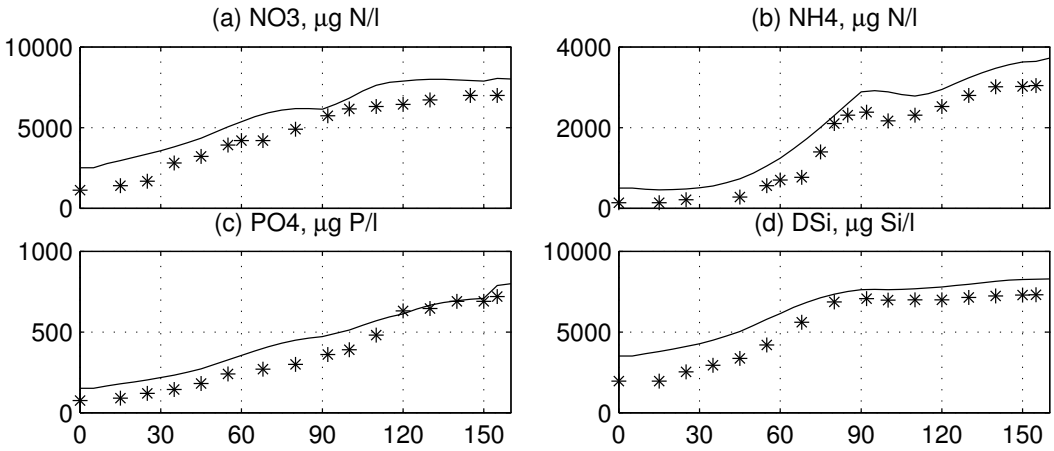

Figure 8: Longitudinal variation of the model simulated nutrients (-) and measurements (*) for the year 2003. X-axis is in kms, with 0 km at Vlissingen and 160 km at Ghent. The three main rivers Rupel, Durme and Dender join the Scheldt river at around 92, 100 and 123 kms, respectively from Vlissingen.

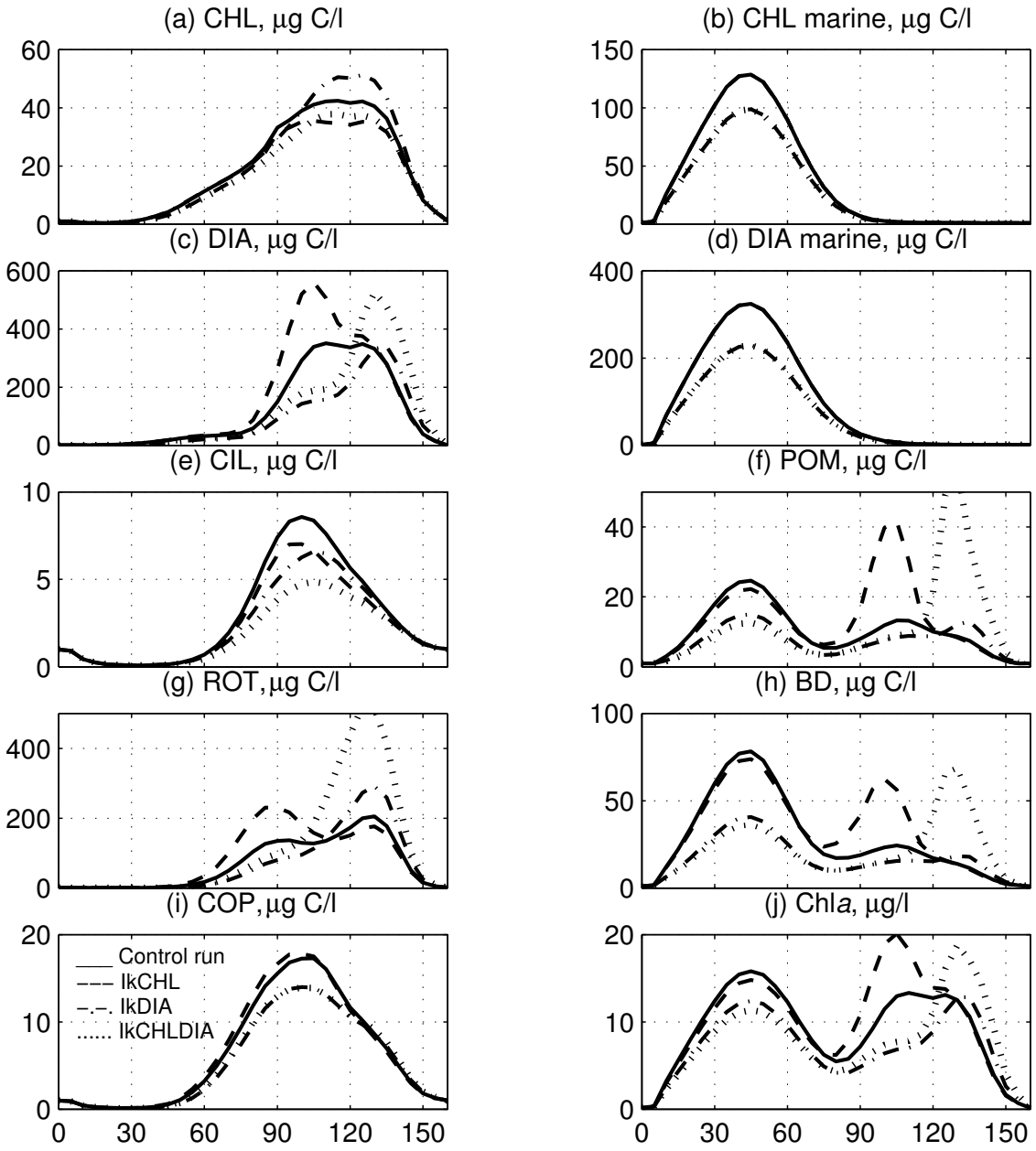

Figure 9: Longitudinal variation of model simulated variables with light saturation constant for phytoplankton changed separately or simultaneously (I_{kCHL} = 125 $\mu mol\ m^{-2}\ s^{-1}$ and I_{kDIA} = 75 $\mu mol\ m^{-2}\ s^{-1}$). X-axis is in kms, with 0 km at Vlissingen and 160 km at Ghent.

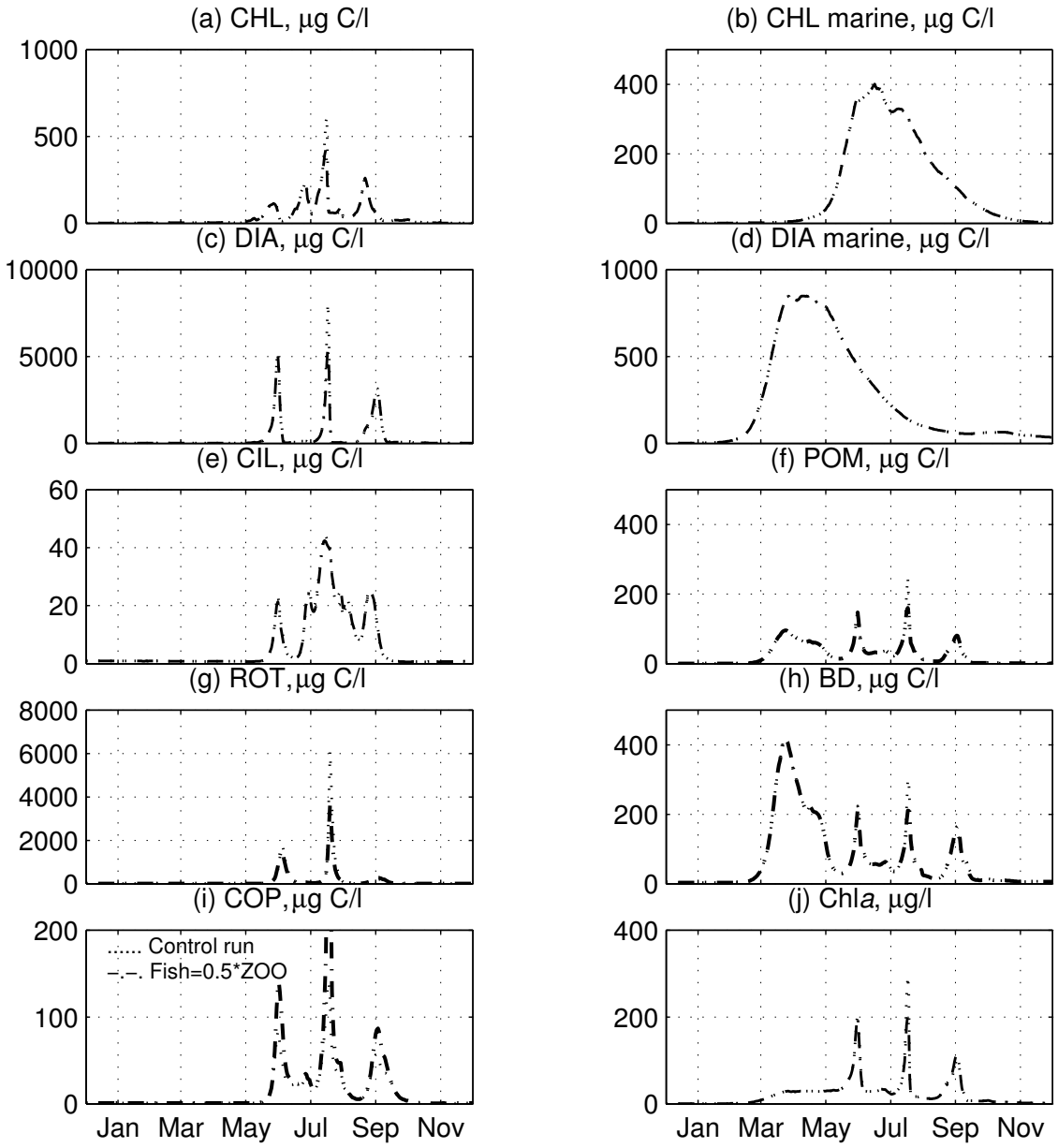

Figure 10: Time series of model simulated variables when the fish biomass was reduced.

Table 1: Variables and parameters for the SLIM model

Parameter	Units
t, the time	s
x, along-river distance	m
A, the cross-section area	m^2
u, the cross-section averaged velocity	d^{-1}
η, the elevation of the free surface above the reference level	m
H, the total effective depth	m
g, the gravitational acceleration	ms^{-2}
ν, the horizontal eddy viscosity	ms^{-2}
C_h, the Chézy coefficient	
k, the longitudinal diffusivity	m^2s^{-1}
C, the tracer concentration	

Table 2: Parameter values for the ecological model

Parameter	Value
General	
dt, time step	$20 minutes$
k_{e1}, background extinction for water	0.2 m^{-1}
k_{e2}, extinction due to SPM	0.02 $L\ mg^{-1} m^{-1}$
I_k, optimum light intensity for phytoplankton	$\mu mol\ m^{-2}\ s^{-1}$
I_o, light intensity at the water surface	$\mu mol\ m^{-2}\ s^{-1}$
k_T, temperature coefficient for the growth rate and other temperature dependent rates	0.069 $^{\circ}C^{-1}$
k_{TRESP}, temperature coefficient for the respiration rate	0.045 $^{\circ}C^{-1}$
k_{Trem}, for remineralization	0.1 $^{\circ}C^{-1}$
T, water temperature	$^{\circ}C$
$RESP_{b0}$, maintenance respiration percentage of phytoplankton at 0 °C	0.03 d^{-1}
$RESP_{p0}$, percentage of $GROWTH_{PHYTO}$ respired at 0 °C	0.03
λ, Ivlev constant	0.01 $(\mu gCl^{-1})^{-1} d^{-1}$
$PHYTO_{min}$, the threshold value of phytoplankton biomass below which zooplankton do not graze	10 μgCl^{-1}
$C:Chla$, ratio of carbon to Chlorophyll-a	30 NO DIM
$R_{C:N}$, ratio of carbon to nitrogen	5.88 NO DIM
$R_{C:P}$, ratio of carbon to phosphate	32.25 NO DIM
$R_{C:Si}$, ratio of carbon to silica	2.13 NO DIM
p_{MORT}, percentage of dead organic matter directly remineralised in the water column	0.4 d^{-1}
p_{FEC}, percentage of feces directly remineralised in the water column	0.4 d^{-1}
NIT_0, nitrification rate coefficient at 0 °C	0.0175 d^{-1}
$DENIT_0$, denitrification rate coefficient at 0 °C	0.0075 d^{-1}
Chlorophytes, CHL (μgCl^{-1})	
$_{NO_3CHL}$, half saturation constant for NO_3 uptake by CHL	10 μgNl^{-1}
K_{NH_4CHL}, half saturation constant for NH_4 uptake by CHL	5 μgNl^{-1}
K_{PO_4CHL}, half saturation constant for PO_4 uptake by CHL	0.5 μgPl^{-1}
$GROWTH_{mCHL}$, CHL maximum growth rate constant at 0 °C	0.36 d^{-1}
I_{kCHL}, CHL optimum light intensity	100 $\mu mol\ m^{-2}\ s^{-1}$
$MORT_{0CHL}$, CHL rate constant at 0 °C	0.000025 $(\mu gCl^{-1})^{-1} d^{-1}$
k_{ECECHL}, CHL ratio of extracellular excretion to photosynthesis	0.05
Diatoms, DIA (μgCl^{-1})	

Continued on next page

Table 2 – continued from previous page

Parameter	Value
K_{NO_3DIA}, half saturation constant for NO_3 uptake by DIA	15 μgNl^{-1}
K_{NH_4DIA}, half saturation constant for NH_4 uptake by DIA	5 μgNl^{-1}
K_{PO_4DIA}, half saturation constant for PO_4 uptake by DIA	1 μgPl^{-1}
K_{DSiDIA}, half saturation constant for DSi uptake by DIA	20 $\mu gSil^{-1}$
$GROWTH_{mDIA}$, DIA maximum growth rate constant at 0 °C	0.42 d^{-1}
I_{kDIA}, DIA optimum light intensity	50 $\mu mol\ m^{-2}\ s^{-1}$
$MORT_{0DIA}$, DIA rate constant at 0 °C	0.0000025 $(\mu gCl^{-1})^{-1}d^{-1}$
k_{ECEDIA}, DIA ratio of extracellular excretion to photosynthesis	0.05
Marine Chlorophytes, CHLM (μgCl^{-1})	
K_{NO_3CHLM}, half saturation constant for NO_3 uptake by CHLM	10 μgNl^{-1}
K_{NH_4CHLM}, half saturation constant for NH_4 uptake by CHLM	5 μgNl^{-1}
K_{PO_4CHLM}, half saturation constant for PO_4 uptake by CHLM	0.5 μgPl^{-1}
$GROWTH_{mCHLM}$, CHLM maximum growth rate constant at 0 °C	0.3 d^{-1}
I_{kCHLM}, CHLM optimum light intensity	100 $\mu mol\ m^{-2}\ s^{-1}$
$MORT_{0CHLM}$, CHLM rate constant at 0 °C	0.00005 $(\mu gCl^{-1})^{-1}d^{-1}$
$k_{ECECHLM}$, CHLM ratio of extracellular excretion to photosynthesis	0.05
Marine Diatoms, DIAM (μgCl^{-1})	
K_{NO_3DIAM}, half saturation constant for NO_3 uptake by DIAM	15 μgNl^{-1}
K_{NH_4DIAM}, half saturation constant for NH_4 uptake by DIAM	5 μgNl^{-1}
K_{PO_4DIAM}, half saturation constant for PO_4 uptake by DIAM	1 μgPl^{-1}
$K_{DSiDIAM}$, half saturation constant for DSi uptake by DIAM	10 $\mu gSil^{-1}$
$GROWTH_{mDIAM}$, DIAM maximum growth rate constant at $Topt_{DIAM}$	0.7 d^{-1}
I_{kDIAM}, DIAM optimum light intensity	50 $\mu mol\ m^{-2}\ s^{-1}$
$MORT_{0DIAM}$, DIAM rate constant at $Topt_{DIAM}$	0.000053 $(\mu gCl^{-1})^{-1}d^{-1}$
$k_{ECEDIAM}$, DIAM ratio of extracellular excretion to photosynthesis	0.05
$Topt_{DIAM}$, optimum temperature for marine diatom growth	8 °C
wt_{DIAM}, width of influence of $Topt_{DIAM}$	10 °C
Ciliates, CIL (μgCl^{-1})	
$RESP_0$, zooplankton respiration rate at 0 °C	0.03 d^{-1}
n_{eZoo}, excretion by zooplankton	0.3
n_{fZoo}, fecal pellet egestion by zooplankton	0.3
$MORT_{0CIL}$, CIL rate constant at 0 °C	0.00025 $(\mu gCl^{-1})^{-1}d^{-1}$
$g_{maxCHLCIL}$, CIL maximum grazing rate constant on CHL at 0 °C	0.4 d^{-1}
Rotifers, ROT (μgCl^{-1})	
$MORT_{0ROT}$, ROT rate constant at 0 °C	0.000003 $(\mu gCl^{-1})^{-1}d^{-1}$

Continued on next page

Table 2 – continued from previous page

Parameter	Value
$g_{maxCHLROT}$, maximum grazing rate constant on CHL by ROT at 0 °C	0.1 d^{-1}
$g_{maxDIAROT}$, ROT maximum grazing rate constant on DIA at 0 °C	0.27 d^{-1}
$p_{maxCILROT}$, ROT maximum grazing rate constant on CIL at 0 °C	0.2 d^{-1}
Copepods, COP (μgCl^{-1})	
$MORT_{0COP}$, COP rate constant at 0 °C	0.00015 $(\mu gCl^{-1})^{-1}d^{-1}$
$g_{maxCHLCOP}$, COP maximum grazing rate constant on CHL at 0 °C	0.1 d^{-1}
$g_{maxDIACOP}$, COP maximum grazing rate constant on DIA at 0 °C	0.25 d^{-1}
$p_{maxCILCOP}$, COP maximum grazing rate constant on CIL at 0 °C	0.1 d^{-1}
$p_{maxROTCOP}$, COP maximum grazing rate constant on ROT at 0 °C	0.15 d^{-1}
Macro-zooplankton or Fish (μgCl^{-1})	
$g_{maxDIAFISH}$, maximum grazing rate constant on DIA by FISH at 0 °C	0.1 d^{-1}
$p_{maxCILFISH}$, maximum grazing rate constant on CIL by FISH at 0 °C	0.1 d^{-1}
$p_{maxROTFISH}$, maximum grazing rate constant on ROT by FISH at 0 °C	0.2 d^{-1}
$p_{maxCOPFISH}$, maximum grazing rate constant on COP by FISH at 0 °C	0.4 d^{-1}
POM (μgCl^{-1}) and BD ($mgCm^{-2}$)	
r_D, remineralization rate constant of POM at 0 °C	0.016 d^{-1}
r_{Ds}, remineralization rate constant of BD at 0 °C	0.016 d^{-1}
k_{Trem}, temperature coefficient for the rate of remineralisation	0.1 $°C^{-1}$
w_{sPOM}, sinking velocity of POM	1.2 md^{-1}

690

Table 3: Percentage change in the ecological variables during various sensitivity tests with I_{kPHYTO} and zooplanktivorous fish population as compared to the control run

Variable	I_{kCHL}	I_{kDIA}	$I_{kCHLDIA}$	$FISH$
	125 $\mu mol\ m^{-2}\ s^{-1}$	75 $\mu mol\ m^{-2}\ s^{-1}$	125 & 75 $\mu mol\ m^{-2}\ s^{-1}$	$FISH = 0.5 * ZOO$
CHL	-12.78	9.07	-13.17	-5.60
$CHLM$	-23.10	-	-23.10	-
DIA	30.85	-25.70	4.17	-6.64
$DIAM$	-	-29.14	-29.14	-
CIL	-15.15	-17.86	-34.57	0.38
POM	28.94	-27.22	11.51	-2.12
ROT	23.86	2.64	69.11	-22.82
BD	16.39	-39.69	-20.97	-1.00
COP	3.42	-14.86	-12.69	46.62
$Chla$	9.05	-21.04	-13.03	-3.15